Residual Phase Noise Modelling of Amplifiers Using Silicon Bipolar Transistors

Konstantinos Theodoropoulos and Jeremy Everard
Department of Electronics
University of York
Heslington, York, YO10 5DD, UK
Email: kt8@ohm.york.ac.uk

Abstract **This paper describes the modelling of residual $1/f$ phase noise for Si bipolar amplifiers operating in the linear region. We propose that for Si bipolar amplifiers the $1/f$ phase noise is largely due to the base emitter recombination flicker noise. The up conversion mechanism is described through linear approximation of the phase variation of the amplifier phase response by the variation of the device parameters (C_{bc}, C_{be}, g_m, r_e) caused by the recombination $1/f$ noise. The amplifier phase response describes the device over the whole frequency range of operation where the influence of the poles and zeros is investigated. It is found that for a common emitter amplifier it is sufficient to only incorporate the effect of the device poles to describe the phase noise behaviour over most of its operational frequency range. Simulations appear to more accurately predict the measurements of others.**

I. Introduction

Amplifier residual phase noise (PM) is one of the most important factors that affect the signal purity of oscillators. While amplitude noise (AM) is a less critical factor in oscillator applications due to the limiting of the amplifier. Both PM and AM noise are the result of up converted baseband flicker noise to the carrier frequency through the device non linear mechanisms [1]–[6].

Several groups have used different approaches for the modelling of the phase noise of Si bipolar amplifiers. In [3], [4] a non linear model based on the charge control model was used. This incorporates the generation of the flicker noise of the device as flicker perturbations in the emitter depletion area and the base width. The model was used as the basis for extensive modelling of various amplifier configurations. In [5] the current noise source approach was adopted to model the flicker noise of the device. A Taylor series method was used to model the variation of the phase transfer function of the amplifier from the change in the bias conditions due to the flicker noise and calculate the PM noise. The model was limited only to the case of a strong Miller effect and the dominant pole approximation was used. Although good agreement was demonstrated up to the $3dB$ point of the amplifier, the measured PM noise at high carrier frequencies (above f_{3dB}) started increasing again. That behaviour was attributed in [5] to the influence of the 2nd pole, however non of the existing models [1]–[6] predicts it. A sensitivity method was introduced in [1], [2] that describes the PM and AM sensitivity of an amplifier in the presence of an independent base band current noise. The method was applied to frequencies below the $3dB$ point where a dominant pole approximation with a strong Miller effect was assumed. In [6] the sensitivity method extended to HBT amplifiers operating at higher frequencies without the dominant pole approximation.

In this work we present a model that attributes the amplifier phase noise to the modulation of the device current dependent parameters by the low frequency flicker noise sources. The examination of a single noise source across the base emitter contact is investigated, since it is accepted in the literature that this is the dominant source of flicker noise in bipolar transistors. A common emitter amplifier is used as a test vehicle where its phase noise is described by its poles and zeros, where the influence of them in the phase noise of the amplifier is characterised. Finally the phase noise characteristics of broadband feedback amplifiers are investigated.

II. Phase Noise Model of Si BJT Amplifiers

For any silicon bipolar amplifier its phase and amplitude transfer function are related to the internal transistor parameters, the external components and the topology. From the internal parameters, some are dynamic and related to the operating conditions of the amplifier, set by the bias current and voltage. The device base emitter low frequency flicker noise modulates the dynamic parameters of the amplifier. This modulation results in the modulation of phase response of the amplifier and thereby modulation of the amplifier output signal, which is described by its phase noise in the Fourier spectrum. Since the amplifier phase transfer function $\varphi(\omega)$ is continuous and since the base emitter noise is very small compared to the base bias current, the variation of the amplifier phase response $\partial\varphi(\omega)$ due to the noise can be evaluated using linear approximation by the use of parametric differentiation with the help of chain rule.

In the work presented here only the influence of the parameters C_{bc}, C_{be}, g_m, r_e will be taken account since are the ones that in various combinations have been used in previous works [1]–[6], while the rest of the device parameters will be regarded as constant. Deriving the phase response $\varphi(\omega)$ of a silicon bipolar amplifier and using the definition that the phase noise $\mathcal{L}(\omega)$ is half of the phase fluctuations spectrum [8], the phase noise of any silicon bipolar amplifier under linear conditions is given by (1). Where Si_{ben} is the power spectral

978-1-4244-3510-4/09/$25.00

density (PSD) of the base emitter flicker noise current.

$$\mathcal{L}(\omega) = \frac{1}{2}\frac{|\partial\varphi(\omega)|^2}{BW} = \frac{1}{2}\frac{1}{BW}\left|\frac{\partial\varphi(\omega)}{\partial C_{bc}}\frac{\partial C_{bc}}{\partial I_C}\frac{\partial I_C}{\partial i_{ben}} + \frac{\partial\varphi(\omega)}{\partial C_{be}}\frac{\partial C_{be}}{\partial I_C}\frac{\partial I_C}{\partial i_{ben}} + \frac{\partial\varphi(\omega)}{\partial r_e}\frac{\partial r_e}{\partial I_C}\frac{\partial I_C}{\partial i_{ben}}\right|^2 Si_{ben} \quad (1)$$

III. CE Amplifiers Phase Noise Modelling

The technique described previously will be now applied to a common emitter amplifier stage with and without series feedback, Fig. 1. The biasing representation of the amplifier has been simplified to accommodate different biasing schemes, for example R_{bias} will represent the Thevenin equivalent bias impedance if a voltage divider is used for the input biasing, and V_{bb} the equivalent Thevenin voltage. R_{base} is added for comparison reasons, since it has been used both in [1] and [5].

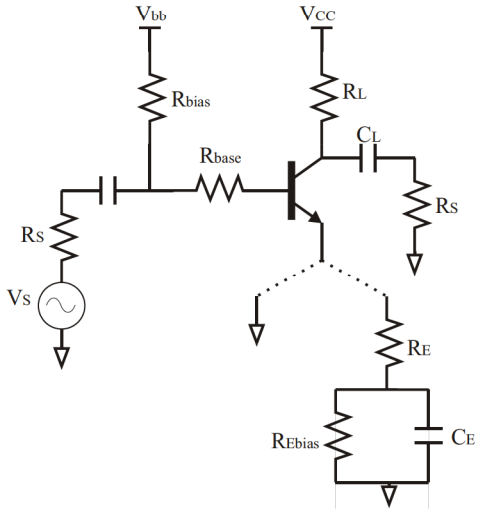

Fig. 1: Common emitter Amplifier Configuration, with and without series feedback

In order to calculate the transfer function of the amplifier for the two configurations the frequency response of the common emitter amplifier with series feedback will be calculated first (r_{ex} is incorporated in R_E), and then by setting $R_E = r_{ex}$ the transfer function of the common emitter stage will be obtained. The equivalent high frequency model of the amplifier is given in Fig. 2. The output resistance of the amplifier r_o usually has a very large and for that reason both has been excluded from the AC model. The load and the collector resistances are combined in R_{Lo} ($R_L//R_C$) and the base external resistance with the base internal parasitic base spread resistance are presented as R_{bb} ($R_{base} + r_{bb}$).

With the use of nodal analysis and the aid of Maple symbolic solver the complete transfer function was calculated

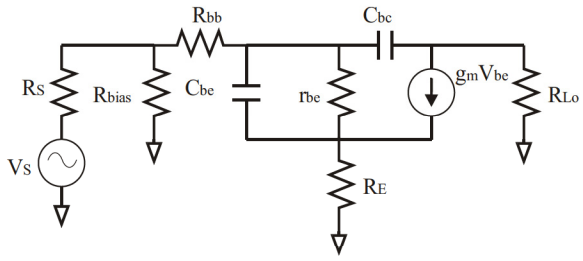

Fig. 2: CE amplifier high frequency hybrid π model

as:

$$\frac{Vc}{Vs} = \frac{G_o\left[(1 - sC_{bc}(r_e + R_E) - s^2C_{be}C_{bc}R_Er_e)\right]}{1 + s\,|G_o|\,(C_{bc}R_{bc} + C_{be}R_{be}) + s^2C_{bc}C_{be}\,|G_o|\,R_{ce}} \quad (2)$$

$$G_o = \frac{-R_{Lo}}{R_E + r_e + \frac{R_B}{(\beta+1)}} \quad (3)$$

The relation of the equivalent resistances R_{bc}, R_{be}, R_{ce} and R_B are given in Appendix. The phase response of the common emitter amplifier with series feedback is obtained as:

$$\varphi(\omega) = \tan^{-1}(\omega\,|G_o|\,(C_{bc}R_{bc} + C_{be}R_{be})) + \tan^{-1}\left(\omega\frac{C_{bc}C_{be}R_{ce}}{(C_{bc}R_{bc} + C_{be}R_{be})}\right) + \tan^{-1}(\omega C_{bc}(r_e + R_E)) + \tan^{-1}\left(\omega\frac{C_{be}R_Er_e}{(r_e + R_E)}\right) \quad (4)$$

The first term of (4) is the phase ($\varphi_{p1}(\omega)$) due to the first pole of the amplifier the 2nd term the phase ($\varphi_{p2}(\omega)$) from the 2nd pole and the same for the zeros ($\varphi_{z1}(\omega)$, $\varphi_{z2}(\omega)$). Therefore the phase noise of the amplifier can be written as:

$$\mathcal{L}(\omega) = \frac{1}{2}\frac{1}{BW}\left|\frac{\partial\varphi_{p1}(\omega)}{\partial i_{ben}} + \frac{\partial\varphi_{p2}(\omega)}{\partial i_{ben}} + \frac{\partial\varphi_{z1}(\omega)}{\partial i_{ben}} + \frac{\partial\varphi_{z2}(\omega)}{\partial i_{ben}}\right|^2 Si_{ben} \quad (5)$$

The current dependent parameters and hence noise dependent of the amplifier are r_e, C_{bc}, C_{be}. The intrinsic dynamic resistance r_e scales with the current as $r_e = \frac{V_T}{I_C}$. The base emitter capacitance C_{be} is the equivalent capacitance of C_b and C_{je}. The base charging capacitance C_b relates to the current as $C_b = \frac{I_C}{V_T}\tau_f$ where τ_f is the forward transit time, τ_f is calculated using the spice model equation in [9]. The forward transit time is current dependent and voltage dependent [9], [10], but since its value is much smaller than $\frac{I_C}{V_T}$ its modulation effect is assumed to be negligible. The base emitter depletion capacitance C_{je} is also much smaller than C_b and therefore its modulation is ignored, while it's value is calculated from the spice model equation in [9]. Therefore C_{be} is calculated as $C_{be} = \frac{I_C}{V_T}\tau_f + C_{je}$. The base collector capacitance C_{bc} is

related with the base collector voltage as [10]:

$$C_{bc} = \frac{C_{jC}}{\left(1 - \frac{V_{BC}}{V_{jC}}\right)^{M_{JC}}} \tag{6}$$

The relationship between the collector current I_C and base collector voltage V_{BC} with the flicker noise current i_{ben} are obtained by the low frequency analysis of the amplifier circuit of Fig. 2, which is the same process used in [3]–[5]. The low frequency equivalent signal is given in Fig 3, where Z_E, Z_B and Z_L are the Thevenin equivalent impedances and their expressions are given in Appendix.

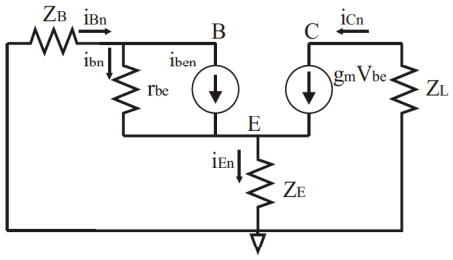

Fig. 3: Simplified low frequency model of the common emitter amplifier with emitter degeneration for noise analysis

$$i_{Cn} = -i_{ben} \cdot \frac{(Z_E + Z_B)}{Z_E + r_e + \frac{Z_B}{\beta+1}} \tag{7}$$

$$v_{BCn} = i_{ben} \cdot \left[\frac{Z_B\,(Z_E + r_e) + Z_L\,(Z_E + Z_B)}{Z_E + r_e + \frac{Z_B}{\beta+1}}\right] \tag{8}$$

In order to calculate the phase noise of the amplifier the partial derivates need to be calculated for each pole and zero. Adding the products of the partial derivates the complete phase noise equation was calculated. Also the effect of each pole and zero in the phase noise of the amplifier can independently investigated, in order to decide the optimal complexity for the phase noise equation. Therefore the phase noise due to the first pole and due to both poles will be calculated respectively as:

$$\mathcal{L}(\omega)_{p1} = \frac{1}{2}\frac{1}{BW}\left|\frac{\partial\varphi_{p1}(\omega)}{\partial i_{ben}}\right|^2 Si_{ben} \tag{9}$$

$$\mathcal{L}(\omega)_{p1p2} = \frac{1}{2}\frac{1}{BW}\left|\frac{\partial\varphi_{p1}(\omega)}{\partial i_{ben}} + \frac{\partial\varphi_{p2}(\omega)}{\partial i_{ben}}\right|^2 Si_{ben} \tag{10}$$

In the same way the phase noise can be obtained due to the poles and the first zero ($\mathcal{L}(\omega)_{p1p2z1}$) and for all poles and zeros ($\mathcal{L}(\omega)_{p1p2z1z2}$). Finally it is important to mention that the transposed mechanism of the flicker noise (partial derivatives) is independent of the flicker noise source PSD (Si_{ben}) (9), therefore a test noise source with reasonable values can be used to investigate the behaviour of various amplifiers.

IV. Phase Noise Equations Evaluation

In order to evaluate the different phase noise equations a test amplifier was designed using the npn bipolar transistor BFS17, Fig. 4. The PM noise modelling equations are compared with the harmonic balanced simulator of Agilent advanced design system (ADS) which has shown to accurately predict the phase noise of oscillators and amplifiers [7]. The amplifier biasing was done with a potential divider, where the equivalent bias resistance R_{bias} has been set deliberately to be of high value so that $R_{bias} >> R_S$, in order to avoid any loading effects and also to ensure that not a low impedance path will be present at low frequencies, that may filter the base emitter flicker noise in a level that the collector emitter flicker noise source has an effect on the phase noise of the amplifier. The amplifier was biased for an I_C of 20 mA and V_{CE} of 5 V, the device internal parameters where calculated from the device spice data ($C_{be} = 81.5\,\text{pF}$, $C_{bc} = 0.49\,\text{pF}$, $r_{ex} = 0.3\,\Omega$, $r_{bb} = 10\,\Omega$). For the flicker noise model (11) the following coefficients have been used, $AF = 2.2$, $kF = 6.58 \cdot 10^{-10}$ and $b = 1$. For the simulation the package parasitics have been excluded since their influence is not accounted in the present model.

$$Si_{ben} = Kf\frac{I_B^{AF}}{f^b} \tag{11}$$

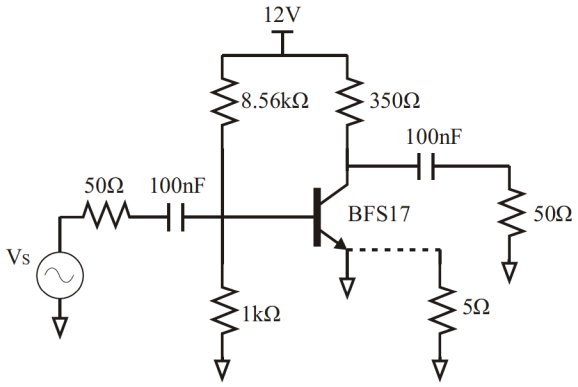

Fig. 4: Common emitter amplifier using BFS17 NPN transistor

Initially the amplifier phase noise was calculated without series feedback (emitter to ground), in which case the phase noise due to the 1st pole $\mathcal{L}(\omega)_{p1}$, the two poles $\mathcal{L}(\omega)_{p1p2}$, and the poles and zero $\mathcal{L}(\omega)_{p1p2z1}$ are calculated at 10 Hz offset from carrier and plotted vs. carrier frequency, the model plots are then compared with the ADS simulated noise, Fig. 5. The modelled phase noise shows excellent agreement with the simulation for, $\mathcal{L}(\omega)_{p1p2}$ and $\mathcal{L}(\omega)_{p1p2z1}$, while $\mathcal{L}(\omega)_{p1}$ at frequencies above f_{3dB} (PM noise first peak) starts diverging, at that point the influence of the 2nd pole comes to effect and the noise starts rising again, while the phase noise due to the zero seems to have little to no effect. Especially for the frequency region up to the $0dB$ gain (1.85 GHz) the modelled phase noise that accounts for the influence of the two pole is adequate.

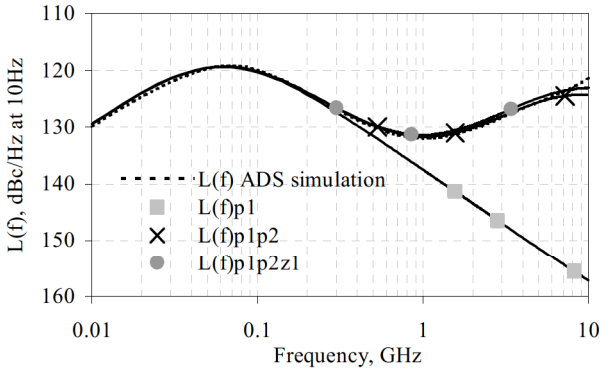

Fig. 5: Common emitter amplifier phase noise at 10 Hz offset from carrier vs. carrier frequency, modelled phase noise for the different contributions of the poles and the zero compared with ADS simulation

A similar behaviour is observed when a series RF feedback is added on the circuit ($R_E = 5\,\Omega$, I_C of 20 mA and V_{CE} of 5 V), Fig. 6, the feedback has the effect of moving the poles closer together, making the impact of the 2nd pole more profound. The single pole equation starts diverging above f_{3dB} more rapidly than before. The equation that accounts for all poles and zeros is the only one that predicts a different behaviour. This is the result of the initial assumption that the zeros are well separated, in that case the approximation gives incorrectly the value of the 2nd zero at 1.6 GHz and shows increased impact on the phase noise. Again it can be shown that up to the frequency of $0dB$ gain (1.7 GHz) the influence of the two poles is sufficient to model the phase noise of the amplifier.

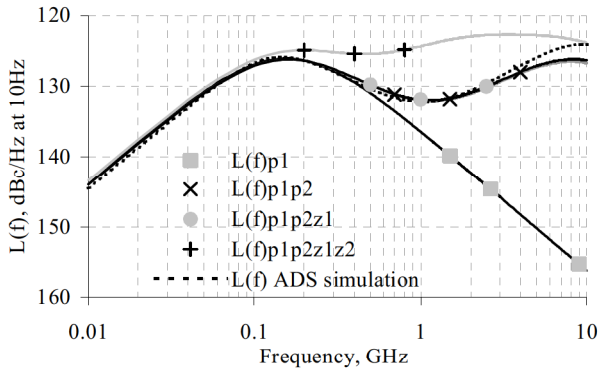

Fig. 6: Common emitter amplifier with series feedback ($R_E = 5\,\Omega$) phase noise at 10 Hz offset from carrier vs. carrier frequency, modelled phase noise for the different contributions of the poles and the zeros compared with ADS simulation

The effect of the series RF feedback on the phase noise of the amplifier can be observed in Fig. 7 where for frequencies below f_{3dB} the feedback resistor improves the phase noise characteristics of the amplifier substantially while at higher frequencies the phase noise starts converging with very small difference between the different cases. Increasing R_E increases the effect of the 2nd pole on the amplifier phase noise, this results that the noise after f_{3dB} to start flattening which explains the results of [5]. Observing how the gain of the amplifier varies with frequency, Fig. 8, it can be seen that most of the reduction of the phase noise comes from the high frequency linearization of the amplifier while a smaller percent can be attributed on the linearization of it's dc characteristics, which agrees with [3], [4]. What needs to be mentioned, is that the package parasitics of the device will probably have an increased effect on the influence of the 2nd pole something that has not be taken in account on the present model.

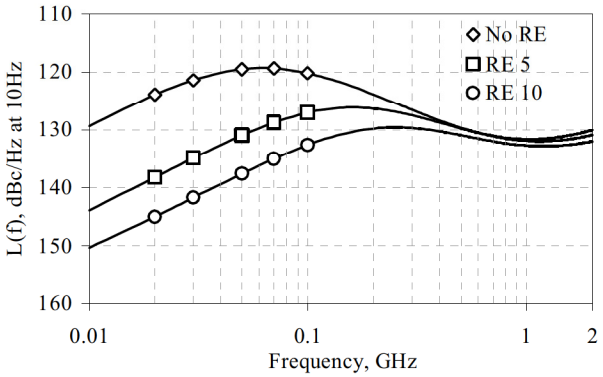

Fig. 7: Common emitter amplifier at 10 Hz offset from carrier vs. carrier frequency, $\mathcal{L}(\omega)_{p1p2}$ for R_E 0 Ω, 5 Ω and10 Ω (I_C 20 mA and V_{CE} 5 V)

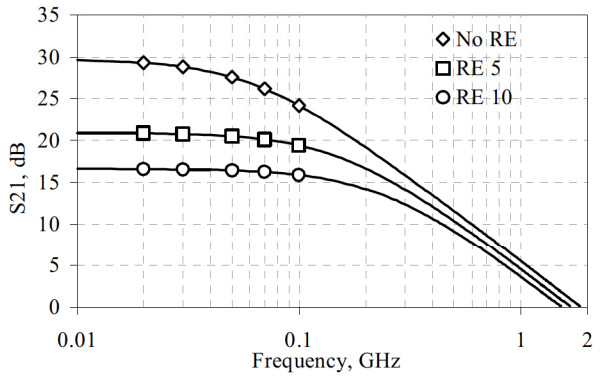

Fig. 8: Common emitter amplifier S_{21} vs. frequency for R_E 0 Ω, 5 Ω and 10 Ω (I_C 20 mA and V_{CE} 5 V)

V. Comparison of Phase noise Equations with Independent measured data

In order to further validate the proposed amplifier phase noise model the CE amplifier presented in [5] and the independent measurement data provided are compared for the phase noise models (9) and (10). The device and amplifier parameters are taken from [5], [11], and the Spice model of the device (BFQ17 NPN bipolar transistor). In Fig. 9 it

is shown, the measured amplifier phase noise at frequency offsets of 10 Hz and 40 Hz vs. carrier frequency, compared with (9) and (10). The measured amplifier peak is at 40 MHz while the modelled is at 46 MHz, this has a result of a slight shift towards higher frequencies of the modelled PM noise, moreover at the frequencies above f_{3dB} the measured PM noise appears to flatten faster due to the influence of the 2nd pole of the device, a behaviour predicted from (10) but at a higher frequency offsets. The reason for that deviation can be attributed to the effect of the device parasitics on the amplifier, since the actual 2nd pole of the device is at about 1 GHz and the ideal modelled one is at 3 GHz, the effect of the device parasitics is also the result of the small miscalculation of the frequency first noise peak. A complete comparison with all the data provided in [5] is shown at Fig. 10.

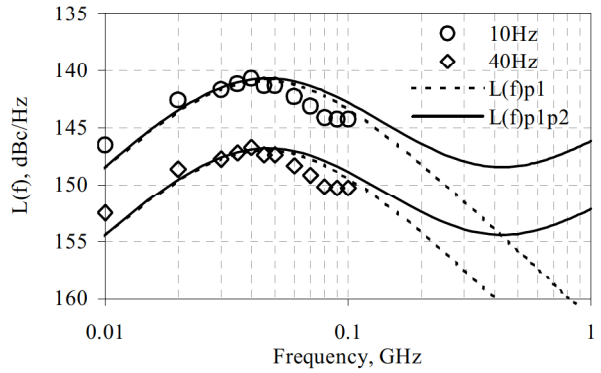

Fig. 9: Comparison of a CE amplifier phase noise at 10 Hz and 40 Hz offsets vs. carrier frequency for the measured independent data and the modelled PM noise taking the effect of the two poles $\mathcal{L}(\omega)_{p1p2}$ and the single pole $\mathcal{L}(\omega)_{p1}$.

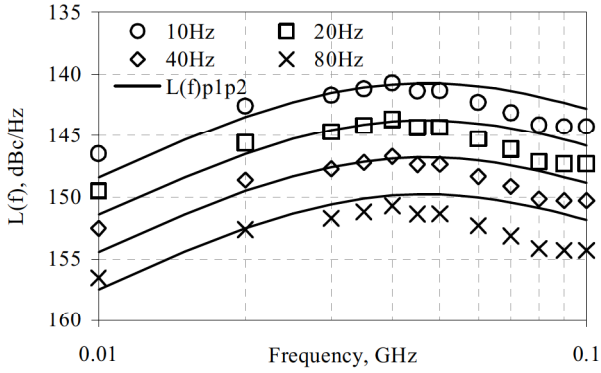

Fig. 10: Comparison of the CE amplifier measured phase noise at 10 Hz, 20 Hz, 40 Hz, and 80 Hz offsets vs. carrier frequency with $\mathcal{L}(\omega)_{p1p2}$.

VI. Broadband Amplifiers Phase Noise Characteristics

In previous sections the common emitter configuration with series feedback has been investigated, however such a topology is not used for microwave design for the reason that although the feedback improves the bandwidth of the amplifier, the input impedance is optimal for a voltage match and offers a very poor power match to 50 Ω. In order to improve both the input and output match of the amplifier and achieve broadband gain a different topology is used, Fig. 11, that employs both series and parallel feedback [12]. It is probably obvious that such a topology will provide better phase noise characteristics than the common emitter amplifier with no feedback, however it is interesting to investigate if the parallel feedback resistor R_F improves the phase noise of the amplifier.

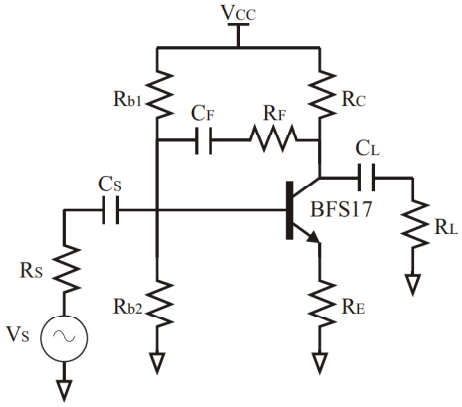

Fig. 11: Broadband amplifier with resistive bias, C_F acts as a DC block

The broadband amplifier PM noise was modelled using the same approach for the CE amplifier. Since for a broadband amplifier the frequency of interest is inside the $3dB$ bandwidth of the amplifier, the PM noise can be modelled only for the influence of the first pole with reasonable accuracy.

To examine the PM noise behaviour of the broadband amplifier, R_E and R_F calculated from the theory described in [12] for the gains of $6dB$, $8dB$, $10dB$ and $12dB$ respectively and for the bias conditions of $I_c = 20\,\text{mA}$ and $V_{CE} = 5\,\text{V}$. Initially the modelled phase noise of the broadband amplifier was calculated for an S_{21} of 12 dB ($R_E = 8.5\,\Omega$, $R_F = 249\,\Omega$) and is compared with the a common emitter amplifier with a series feedback of the same R_E value and the amplifier without feedback under the same bias conditions, Fig.12. Although the emitter resistance provides a large reduction of the phase noise of the amplifier of about $20dB$ at low carrier frequencies, the addition of the parallel resistance R_F improves the phase noise of the amplifier by an additional $8dB$. That improved suppression of the noise can be attributed to the further linearization that R_F provides on the frequency response of the amplifier in contrast with R_E that also has an effect on the dc gain linearization. Therefore it can be expected that the amount of reduction on the PM noise for lower gains will be about the gain difference. This behaviour is shown at Fig. 13, where the phase noise of the amplifier for a gain of $6dB$, $8dB$, $10dB$ and $12dB$ is plotted and a noise reduction of about $2dB$ per stage is observed.

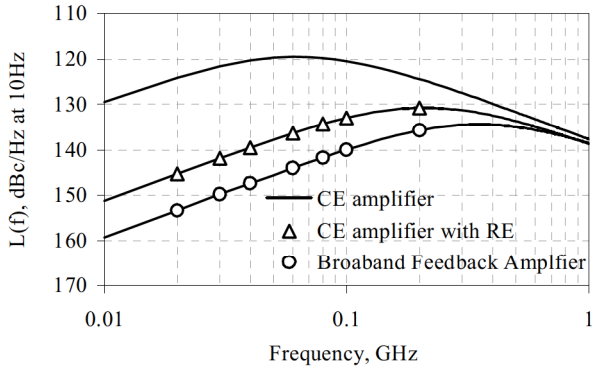

Fig. 12: Modeled phase noise at 10 Hz carrier offset vs carrier frequency for a broadband amplifier with a gain of $12dB$ vs common emitter amplifier with and without series feedback

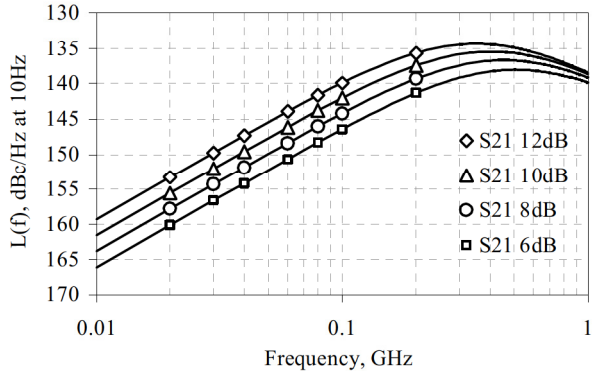

Fig. 13: Modeled phase noise at 10 Hz offset from carrier vs carrier frequency for broadband amplifiers of gain $6dB$, $8dB$, $10dB$ and $12dB$

VII. Conclusions

A modelling technique that describes the phase noise of silicon bipolar amplifiers has been developed. The influence of the poles and zeros on the phase noise of the amplifier has been investigated. It was shown in the models that it is only necessary to include the amplifier poles to describe the phase noise inside its operational frequency range. Good agreement has been observed between the model and independently measured data. However in future models, the effect of the device parasitics will have to be included since they affect the position of the 2nd pole of the amplifier.

Acknowledgment

The Authors would like to thank BAE systems, the Royal Academy of Engineering and the University of York for supporting this work.

Appendix

The common emitter amplifier transfer function symbolic resistances relations are given as:

$$R_{bc} = (R_B + R_E + r_e) + \frac{R_B}{R_{Lo}}(r_e + R_E) \quad (12)$$

$$R_{be} = \frac{r_e}{R_{Lo}}(R_E + R_B) \quad (13)$$

$$R_{ce} = \frac{r_e}{R_{Lo}}(R_E R_B + R_E R_{Lo} + R_B R_{Lo}) \quad (14)$$

$$R_B = (R_s // R_{bias}) + R_{bb} \quad (15)$$

The low frequency equivalent impedances for noise analysis.

$$Z_B = R_{bb} + \frac{R_{bias}\,(1 + j2\pi f_L R_S C_S)}{1 + j2\pi f_L\,(R_S + R_{bias})\,C_S} \quad (16)$$

$$Z_E = R_E + \frac{R_{Ebias}}{1 + j2\pi f_L R_{Ebias} C_E} \quad (17)$$

$$Z_L = \frac{R_C\,(1 + j2\pi f_L R_L C_L)}{1 + j2\pi f_L\,(R_L + R_C)\,C_L} \quad (18)$$

f_L describes the frequency range where the low frequency noise of the device has $1/f$ characteristics.

References

[1] F. L. Walls, E. S. Ferre-Pikal, and S. R. Jefferts, "Origin of 1/f PM and AM noise in bipolar junction transistor amplifiers," IEEE Trans. Ultrason., Ferroelect., Freq. Contr., vol. 44, no. 2, pp. 326 334, March 1997.

[2] E. S. Ferre-Pikal, F. L. Walls, and C. W. Nelson, "Guidelines for designing BJT amplifiers with low 1/f AM and PM noise," IEEE Trans. Ultrason., Ferroelect., Freq. Contr., vol. 44, no. 2, pp. 335 343, March 1997.

[3] V. N. Kuleshov and T. I. Boldyreva, "1/f AM and PM noise in bipolar transistor amplifiers: Sources, ways of influence, techniques of reduction," in Proc. IEEE Int. Freq. Contr. Symp., pp. 446 455, May 1997.

[4] V. N. Kuleshov, "1/f models of bipolar junction transistor and their application to PM and AM noise calculation," in Proc. IEEE Int. Freq. Contr. Symp., pp. 164 171, May 1998.

[5] T.-D. Tomlin, K. Fynn, and A. Cantoni, "A model for phase noise generation in amplifiers," IEEE Trans. Ultrason., Ferroelect., Freq. Contr., vol. 48, no. 6, pp. 1547 1554, November 2001.

[6] E. S. Ferre-Pikal and and F. H. Savage, "Up-converted 1/f pm and am noise in linear HBT ampliers," IEEE Trans. Ultrason., Ferroelect., Freq. Contr., vol. 55, no. 8, August 2008.

[7] L. Eichinger, F. Sischka, G. Olbrich, and R. Weigel, "Simulation and design of rf oscillators, in Proc. 2nd International Symposium on Acoustic Wave Devices for Future Mobile Communication Systems, pp. 67 73, March 2004.

[8] "IEEE standard definitions of physical quantities for fundamental frequency and time metrology - random instabilities," IEEE Std 1139-1999, July 1999.

[9] P. Antognetti and G. Massobrio, Semiconductor Device Modeling with Spice, 3rd ed. McGraw-Hill Professional, 1998., ch. 2.

[10] K. R. Laker, Design of Analog Integrated Circuits and Systems, McGraw-Hill Companies, 1994., ch. 2.

[11] T.-D. Tomlin, "Analysis and modeling of jitter and phase noise in electronic systems: Phase noise in rf ampliers and jitter in timming recovery circuits,"Ph.D. dissertation, The University of Western Australia. School of Electrical and Electronic, and Computer Engineering, January 2004, ch. 4.

[12] J. Everard, Fundamentals of RF Circuit Design: with Low Noise Oscillators, 1st ed. Wiley, 2001., ch. 3.